SUPPLEMENTARY MATERIALS

Kernel-to-ES field translation

The sequential process of translation first involves the ArcGIS Euclidian Distance tool, followed by the Raster Calculator. The Raster Calculator allows algebraic expressions to be carried out using raster layers - a raster refers to a matrix of cells (or pixels) where each cell has an assigned value [1]. This allows the translation of the mathematical formulas developed in Step 1 to each raster grid cell. The analysis of multiple configurations of SPUs of various sizes required by this research exceeded the capability of standard ArcGIS Pro tools. We therefore developed a new stand-alone tool for ArcGIS Pro that provides two developments of the basic toolset. Firstly, this tool allows the input of differently sized SPUs and calculates the impact of SPU area on both kernel intensity and range. Secondly, it allows for variation in the kernel overlap intensity (the standard Raster Calculator only provides simple addition of values for interaction zones). The Python script for this tool is available upon request.

Field quantification

For each spatial configuration of SPU patches, ESFIELD uses GIS to graphically depict the ES fields radiating from respective SPUs. To quantify the ES performance of each configuration, the ArcGIS Pro Zonal Statistics as Table tool (Spatial Analyst) identifies all raster pixels within the research area boundary, whether the pixels are contiguous or not. The raster values of the ES influence fields are summed, including areas of overlap. The sum of individual pixel ES values for each landscape configuration (including the areas occupied by SPUs) provides an overall 'ES Score,' an indication of that configuration's provision of each ES across the research area as a whole. To allow comparison of ES performance between the various configurations, the ES score for each configuration is normalised to a range between 0 and 10, where 10 represents the maximum value measured for the service across all configurations [2, 3].

Kernel development of specific ES.

Cooling effect

The three variables by which vegetation regulates urban temperatures apply also to tree clumps in rural environments: by shading solar radiation, through the process of evapotranspiration and by altering air movement and heat exchange [4]. We therefore propose tree clumps of various sizes as SPUs for the purpose of this research.

Vegetation breezes result from the same physical process behind the urban cooling urban phenomenon in cities, where advection caused by the temperature differential between the cooler park and its warmer (built-up) surroundings can, in some cases, result in the cooling effect of a park dispersing hundreds of meters from the cooling source [5-7]. To apply InVEST to the rural context of our research, the warmer surfaces of pasture are substituted for built-up areas, with cooler tree clumps representing the urban park cooling source. The resulting negative exponential decay of the kernel correlates with empirical evidence observed in urban cooling literature [6, 8-11]. InVEST calculates the cooling effect of urban parks over a cooling distance (dcool) based on the Cooling Coefficient (CC) derived from albedo, evapotranspiration and shading properties assigned to individual tree species, and the area (A) of the urban park (Figure S1) [12]. We adapt this formula by letting A represent the SPU area and assigning a constant CC value to the SPU, given we use a homogenous and generic tree species for the purposes of developing this model

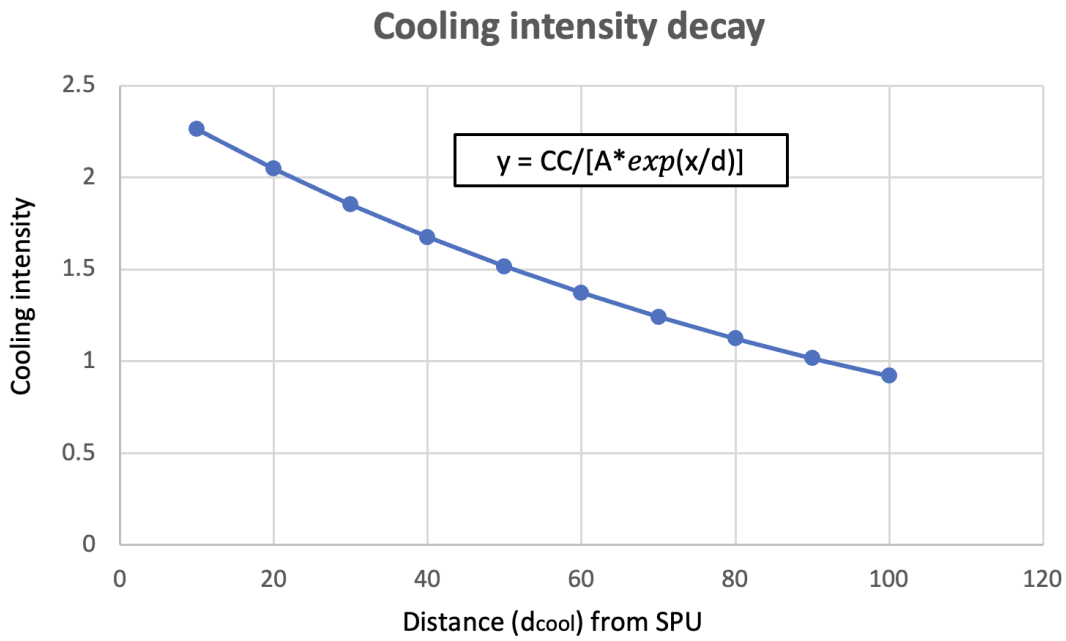

Figure S1. The InVEST model is used to calculate the distance-decay of cooling intensity over a distance (d_{cool}) from the SPU. We apply a constant Cooling Coefficient (CC) value given the homogenous and generic tree species used for the purposes of developing this model. Area (A) is the area of the SPU.

Micrometeorological phenomena characteristic of forest edge context: The specific differentials of surface roughness between forest and clearing (or in our context, tree clump and pasture), in addition to temperature, are shown to result in distinct air circulation patterns [13, 14]. The large-scale convective eddies that are formed manifest as regular ejections of cool air from the forest interior to the clearing [13]. For the purposes of this conceptual model, we propose that in ideal conditions (referring to convective boundary layer conditions and variable wind direction), the distance these jets reach from the forest edge is modelled as a function of the displaced cool air volume that is available in the shaded sub-canopy zone. The intermittency of horizontal wind speeds that advect the cold air outwards is related to the convective turbulence time scale (the thermal updraft time scale that returns cold air back to the surface). The characteristic time periods of these processes vary between 1 min to 10 min and will occur intermittently throughout the daytime period [15]. We will assume that descending air occurring within these time periods will displace a volume of cool air through the clump canopy and the typical height of the sub-canopy space (Figure S2). Neglecting turbulent heat transfer between the warmer ground outside the canopy and the volume of cool air displaced horizontally, we will assume that the displaced cool air will travel a distance of $d_{cool}=2R_{clump}$, occurring over a periodic cycle varying between 1 min and 10 min.

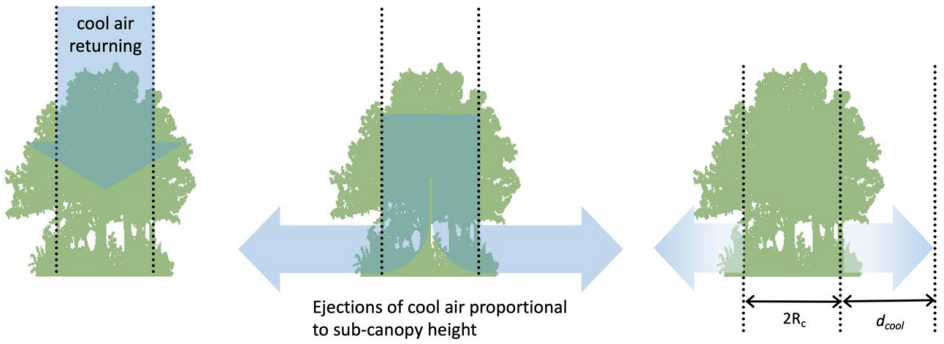

Figure S2. Diagram indicating simplified micrometeorological effects particular to rural tree clumps that support cooling phenomena.

Nitrogen retention

Excessive N in waterways can result in hypoxic conditions and metabolic toxicity, leading to decline of ES and biodiversity [16, 17]. There are also potential risks to human health associated with excessive nitrates in drinking water, the most prominent being colorectal cancer and methemoglobinemia (blue baby syndrome) [18, 19]. Strategic planting of vegetation, such as riparian planting, can be used to intercept surface and sub-surface flows of nutrients and contaminants, including nitrates [20, 21].

Quantifying root distribution pattern is extremely difficult due to high variability between species, changing architecture according to soil characteristics and limitations of present detection methodologies [22-24]. This complexity is partially mitigated by the fact that rhizosphere conditions, rather than plant type, are the primary determinants of root system shape and size [22, 25].

Alder root biomass characteristics: This New Zealand research comprised a randomised field trial with nine exotic tree species, carried out over three years [26]. This included annual measurement of both above- and below- ground metrics, including tree height, canopy spread (i.e., canopy diameter) and spread of lateral roots (mean maximum root length from the trunk). Note that root measurements included only coarse roots (greater than 1 mm in diameter) [26]. We used Alder (Alnus viridis) as the focal species, as it exhibited the greatest root biomass at the end of the 3-year trial. The mat-like architecture of Alder's root system also suggests a high degree of rhizosphere occupancy and therefore contact with sub-surface nitrate flows. The ratio of diameter of lateral root spread to tree height was 1.4 (the sampled species average was 1.2). Based on the total root biomass measured at regular radial distances from the trunk, we determined a mathematical expression for the spatial distribution of root architecture of species used in that research. This is used to develop a kernel expression of an individual plant's ability to intercept subsurface nitrates (Figure S3). The ES field's range for nitrogen retention was the estimated extent of root structure from the perimeter of the SPU – set at seven metres for the purposes of this research, based on a five-metre-high woody vegetation clump.

ES overlap intensity is less clear and needs to be estimated on a species-by-species basis. Different species demonstrate quite different root interaction patterns with neighbouring trees, along a continuum ranging from exclusion to combination [27-29]. For Alder, we assume a high degree of root interweaving (C. J. Phillips, personal communication, 19 September 2022) and therefore assume interception capacity will be additive in areas of overlap.

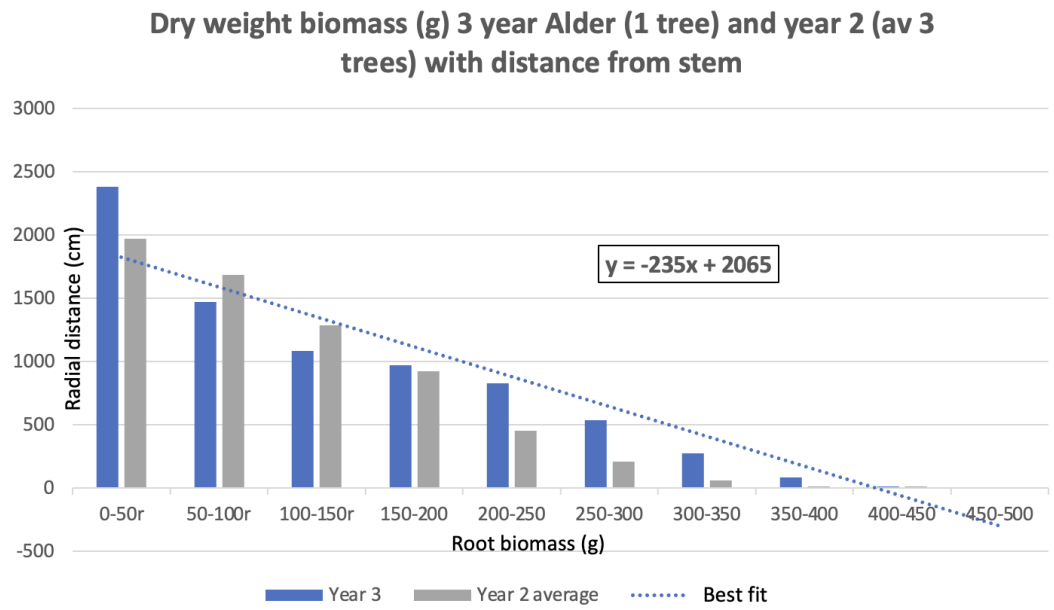

Figure S3. The total root biomass measured at regular radial distances from the trunk was used to determine a mathematical expression for the spatial distribution of root architecture.

Habitat suitability

The piwakawaka (fantail, Rhipidura fugilinosa) and korimako (bellbird, Anthornis melanura) are found throughout New Zealand, and are respectively an insectivore and a nectar-feeder [30, 31]. Piwakawaka prefer forest edge habitats, while korimako require more intact forest to breed [32]. Due to these contrasts, these two species have been identified as potential co-indicators of indigenous ecosystem resilience in New Zealand rural landscapes [32]. The piwakawaka has adapted successfully to landscape fragmentation [33, 34]; it is well-known for its distinctive sallying behaviour when feeding, frequently in close proximity to humans [35, 36]. Korimako prefer intact forest for nesting but will occasionally fly long distances (greater than 500 m) to feed on preferred flowering species [37-39]. We translate data obtained from literature to generate an ES kernel for each species. A nominal population for each species is assigned to the tree clump, which is assumed to comprise tree species that are most conducive for the nesting and feeding of the two species. It is recognised there is a minimum clump area required for the establishment of nesting and establishment of a home range [33]. For korimako, we have set this minimum SPU area to 1.5 ha. Piwakawaka, on the other hand, will nest even in the smallest 0.02 ha SPUs (which translates to a tree clump of 16m diameter), as long as the distance to a neighbouring clump is no greater than 150m. The functional form is based on the triweight kernel used by Laca (2021), considered a reasonable representation of population distribution from nesting site (Figure S4) [40]. Its single parameter λ is the reciprocal of the kernel range, in this context, the feeding range of the subject species (50 m for piwakawaka, 500m for korimako).

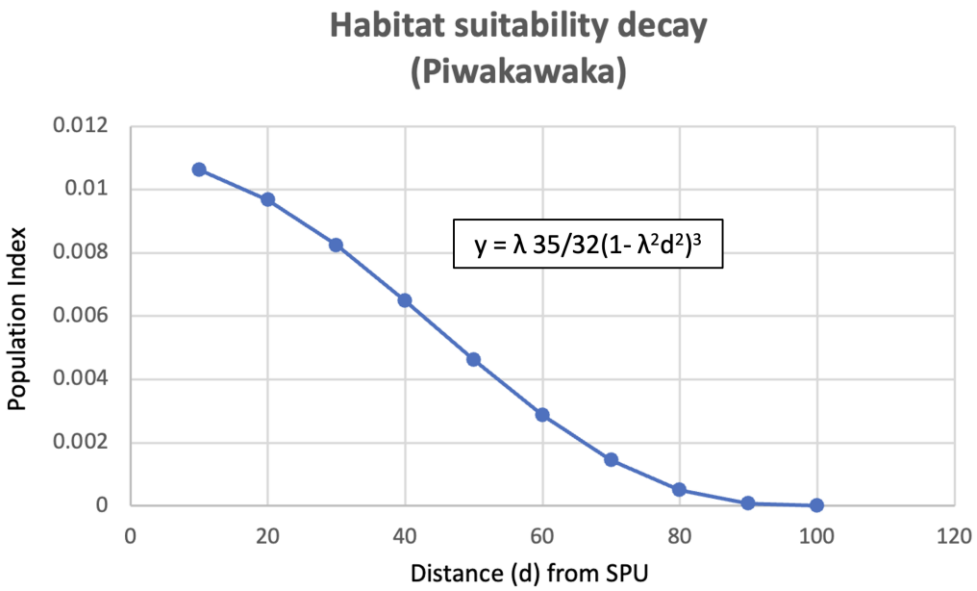

Figure S4. The triweight kernel, shown in this graph, is considered a reasonable representation of population distribution from nesting site. This kernel indicates the distribution of piwakawaka from SPU, where d is assigned a maximum value of 100m, reflecting the nominal maximum feeding range for this species used for the purposes of this research. For korimako, d is increased to 500m.

Supplementary Material References

1. Esri. *Raster Calculator (Spatial Analyst)*. 09/08/2022]; Available from: https://pro.arcgis.com/en/pro-app/2.8/tool-reference/spatial-analyst/raster-calculator.htm.
2. Lamy, T., et al., *Landscape structure affects the provision of multiple ecosystem services.* Environ. Res. Lett, 2016. **11**(12): p. 124017.
3. Spake, R., et al., *Unpacking ecosystem service bundles: Towards predictive mapping of synergies and trade-offs between ecosystem services.* Global Environmental Change, 2017. **47**: p. 37-50.
4. Zardo, L., et al., *Estimating the Cooling Capacity of Green Infrastructures to Support Urban Planning.* Ecosystem Services, 2017. **26**: p. 225-235.
5. Cao, X., et al., *Quantifying the cool island intensity of urban parks using ASTER and IKONOS data.* Landscape and Urban Planning, 2010. **96**(4): p. 224-231.
6. Yin, S., et al., *Spatial-temporal pattern in the cooling effect of a large urban forest and the factors driving it.* Building and Environment, 2022. **209**: p. 108676.
7. Lin, B.-S. and C.-T. Lin, *Preliminary study of the influence of the spatial arrangement of urban parks on local temperature reduction.* Urban Forestry & Urban Greening, 2016. **20**: p. 348-357.
8. Hamada, S., T. Tanaka, and T. Ohta, *Impacts of land use and topography on the cooling effect of green areas on surrounding urban areas.* Urban Forestry & Urban Greening, 2013. **12**(4): p. 426-434.
9. Martini, A., D. Biondi, and A.C. Batista, *Distance and Intensity of Microclimatic Influence Provided by Urban Forest Typologies.* Floresta Ambient, 2018. **25**(2).
10. Lin, W., et al., *Calculating cooling extents of green parks using remote sensing: Method and test.* Landscape and Urban Planning, 2015. **134**: p. 66-75.
11. Honjo, T. and T. Takakura, *Simulation of thermal effects of urban green areas on their surrounding areas.* Energy and Buildings, 1990. **15**(3): p. 443-446.
12. Lonsdorf, E.V., et al., *Assessing urban ecosystem services provided by green infrastructure: Golf courses in the Minneapolis-St. Paul metro area.* Landscape and Urban Planning, 2021. **208**: p. 104022.
13. Eder, F., A. Serafimovich, and T. Foken, *Coherent Structures at a Forest Edge: Properties, Coupling and Impact of Secondary Circulations.* Boundary-layer Meteorology, 2013. **148**(2): p. 285-308.
14. Huang, J., M. Cassiani, and J.D. Albertson, *Coherent Turbulent Structures Across a Vegetation Discontinuity.* Boundary-layer Meteorology, 2011. **140**(1): p. 1-22.
15. Stull, R.B., *An Introduction to Boundary Layer Meteorology*. Atmospheric and Oceanographic Sciences Library. 1988, Dordrecht, Germany: Springer
16. Dodds, W.K. and V.H. Smith, *Nitrogen, phosphorus, and eutrophication in streams.* Inland Waters (Print), 2016. **6**(2): p. 155-164.
17. Camargo, J.A. and Á. Alonso, *Ecological and toxicological effects of inorganic nitrogen pollution in aquatic ecosystems: A global assessment.* Environ Int, 2006. **32**(6): p. 831-849.
18. Knobeloch, L., et al., *Blue babies and nitrate-contaminated well water.* Environmental Health Perspectives, 2000. **108**(7): p. 675-678.
19. Choudhary, M., M. Muduli, and S. Ray, *A comprehensive review on nitrate pollution and its remediation: conventional and recent approaches.* Sustainable Water Resources Management, 2022. **8**(4): p. 113.
20. Parkyn, S., *Review of riparian buffer zone effectiveness* ed. A. New Zealand. Ministry of and Forestry. 2004, Wellington [N.Z.]: Wellington N.Z. : Ministry of Agriculture and Forestry.
21. Haycock, N.E. and G. Pinay, *Groundwater Nitrate Dynamics in Grass and Poplar Vegetated Riparian Buffer Strips during the Winter.* Journal of Environmental Quality, 1993. **22**(2): p. 273-278.
22. Saha, R., et al., *Root distribution, orientation and root length density modelling in Eucalyptus and evaluation of associated water use efficiency.* New Forests, 2020. **51**(6): p. 1023-1037.

23. Dunbabin, V., Z. Rengel, and A.J. Diggle, *Simulating Form and Function of Root Systems: Efficiency of Nitrate Uptake Is Dependent on Root System Architecture and the Spatial and Temporal Variability of Nitrate Supply.* Functional Ecology, 2004. **18**(2): p. 204-211.
24. Marden, M., S. Lambie, and C. Phillips, *Biomass and root attributes of eight of New Zealand's most common indigenous evergreen conifer and broadleaved forest species during the first 5 years of establishment.* New Zealand Journal of Forestry Science, 2018. **48**(1): p. 1-26.
25. Tobin, B., et al., *Towards developmental modelling of tree root systems.* Plant Biosystems, 2007. **141**(3): p. 481-501.
26. Phillips, C.J., M. Marden, and S.M. Lambie, *Observations of "coarse" root development in young trees of nine exotic species from a New Zealand plot trial.* New Zealand Journal of Forestry Science, 2015. **45**(1): p. 1.
27. Mou, P., et al., *Spatial Distribution of Roots in Sweetgum and Loblolly Pine Monocultures and Relations with Above-Ground Biomass and Soil Nutrients.* Functional Ecology, 1995. **9**(4): p. 689-699.
28. Cabal, C., et al., *The exploitative segregation of plant roots.* Science, 2020. **370**(6521): p. 1197-1199.
29. McIvor, I.R., et al., *Structural root growth of young Veronese poplars on erodible slopes in the southern North Island, New Zealand.* Agroforestry Systems, 2007. **72**(1): p. 75-86.
30. Higgins, P.J., J.M. Peter, and S.J. Cowling, *Handbook of Australian, New Zealand & Antarctic birds*. Handbook of Australian, New Zealand and Antarctic birds. 1990, Melbourne: Melbourne : Oxford University Press.
31. Fitter, J., *A field guide to the birds of New Zealand*. Birds of New Zealand, ed. D. Merton and J. Fitter. 2011, Princeton, N.J.: Princeton, N.J. : Princeton University Press.
32. Coleman, G., *Nest site selection of the New Zealand fantail (Rhipidura fugilinosa) on South Island production land*, in *Department of Zoology*. 2008, University of Otago: Dunedin, New Zealand.
33. Meurk, C., G. Hall, and J. Parkes, *Options for enhancing forest biodiversity across New Zealand's managed landscapes based on ecosystem modelling and spatial design.* New Zealand Journal of Ecology, 2006. **30**: p. 131-146.
34. Powlesland, R.G. *New Zealand fantail | pīwakawaka*. New Zealand Birds Online 2022; Available from: www.nzbirdsonline.org.nz.
35. Howe, R.W., *Local dynamics of bird assemblages in small forest habitat islands in Australia and North America.* Ecology (Durham), 1984. **65**(5): p. 1585-1601.
36. Berry, L., *Edge effects on the distribution and abundance of birds in a southern Victorian forest.* Wildlife Research (East Melbourne), 2001. **28**(3): p. 239-245.
37. Spurr, E.B., K.M. Borkin, and S. Rod, *Use of radio telemetry to determine home range and movements of the bellbird (Anthornis melanura) - A feasibility study.* Notornis, 2010. **57**(2): p. 63-70.
38. Anderson, S.H. and J.L. Craig, *Breeding biology of bellbirds (Anthornis melanura) on Tiritiri Matangi Island.* Notornis, 2003. **50**(2): p. 75-82.
39. Spurr, E.B., A.C. Crossland, and P.M. Sagar, *Increased abundance of the bellbird (Anthornis melanura) in Christchurch, New Zealand.* Notornis, 2014. **61**(2): p. 67-74.
40. Laca, E.A., *Multi-Scape Interventions to Match Spatial Scales of Demand and Supply of Ecosystem Services.* Front. Sust. Food Syst., 2021. **4**(289): p. 1-12.

Disclaimer/Publisher's Note: The statements, opinions and data contained in all publications are solely those of the individual author(s) and contributor(s) and not of MDPI and/or the editor(s). MDPI and/or the editor(s) disclaim responsibility for any injury to people or property resulting from any ideas, methods, instructions or products referred to in the content.